

# ENERGY COMPARISON BETWEEN DIFFERENT PARALLEL HYBRID VEHICLES ARCHITECTURES

D. LANZAROTTO, M. PASSALACQUA & M. REPETTO  
University of Genoa, Italy.

## ABSTRACT

A great boom of hybrid vehicles has taken place on the automotive market in recent years, in particular, all these vehicles are now equipped with a continuously variable transmission (CVT) thanks to the use of a planetary gear train and two electric motor-generators.

The benefit provided by this system is the possibility to optimally control the engine velocity from an energy standpoint; in addition, drive comfort is increased thanks to the continuously variable transmission.

However, this is obtained at the cost of some amount of electrical losses in the components necessary to realize the above-mentioned structure.

This paper aims to evaluate the overall efficiency of this particular power train on different road missions; the same missions will be simulated at the same time for an identical hybrid vehicle equipped with a conventional transmission system.

In order to perform an energy analysis of the two architectures, one has to accurately address the main components generating energy losses: it will be thus presented the set of equations from which the mathematical stationary model of the CVT was obtained and how the different electric components and the internal combustion engine were modeled.

In addition, a brief description on the CVT optimization logic will be reported, the validity of this process will be then confirmed by comparing the ICE working points deriving from it and those declared by Toyota.

Finally, the fuel economy values coming from various road simulations will be compared in order to determine if or which hybrid architecture proves to be the most efficient one.

*Keywords:* Continuously variable transmission, Hybrid vehicle, Parallel architecture, Powertrain efficiency

## 1 INTRODUCTION

The current state of art in the automotive sector sees the presence of hybrid vehicles equipped with a continuously variable transmission (CVT) realized with a planetary gear train and two electrical machines (A. Mahmoudi, W. L. Soong, G. Pellegrino and E. Armando). This CVT is made possible by the motor-generator unit connected to the sun gear ( $MGU_1$ ); this component enables the internal combustion engine (ICE), connected to the carrier gear, to rotate at the most suitable velocity.

$MGU_1$  can work both as a generator and as a motor depending on the transmission ratios realized, thus power is exchanged with the electrical machine connected to the ring gear ( $MGU_2$ ) by a fixed-speed reduction gear.

In addition, the storage system allows regenerative deceleration and pure electric traction.

The CVT makes possible an optimal management of the ICE velocity; however, in order to work it creates electrical power circulation between the two motor generator units with its consequent losses.

It is thus of primary importance to analyze the electrical machines and their inverter efficiency because of the fundamental role of the electric components. This study was conducted in (T. A. Burrell, C. L. Coomer, S. L. Campbell, L. E. Seiber, L. D. Marlino, R. H. Staunton, and J. P. Cunningham) for a 2007 Toyota Camry, in (T. A. Burrell, C. L. Coomer, S. L. Campbell, A. A. Wereszczak, J. P. Cunningham, L. D. Marlino,) for a 2008 Toyota Lexus and in (T. A. Burrell,

S. L. Campbell, C. L. Coomer, C. W. Ayers, A. A. Wereszczak, J. P. Cunningham, L. D. Marlino, L. E. Seiber, H. T. Lin) for a 2010 Toyota Prius.

Discontinuously variable transmission (DVT) is the alternative to the above-mentioned structure, this configuration is not able to optimally manage the ICE working conditions as well as the previous structure does; however, this transmission solution is free from any electrical losses which are only associated with regenerative deceleration and electric traction.

The aim of this paper is to evaluate the power train energy efficiency over different working conditions in order to point out the most virtuous solution from an energy efficiency standpoint.

## 2 HYBRID POWERTRAIN

A logical scheme of the two architectures taken into consideration is shown in Fig. 1, the two inverters are included in the 'inverter block' (only in the CVT solution) and the DC/DC converter related to the battery.

In order to briefly present the optimization process regarding the choice of the optimal transmission ratio according to road variables, the power flow scheme of CVT architecture is shown in Fig. 2 (the power flows are to be considered positive if in accordance with the arrow direction).

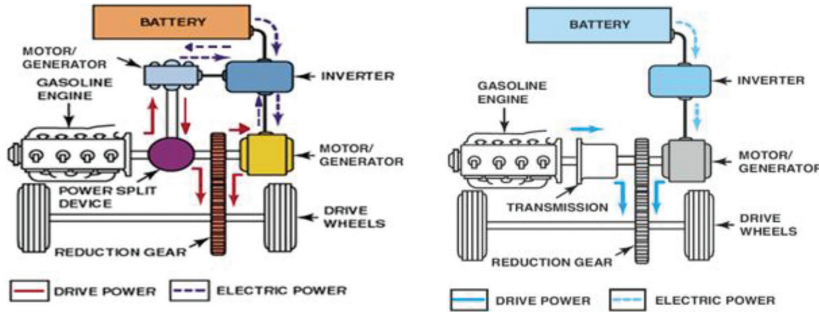


Figure 1: CVT (left) and DVT (right) chitectures.

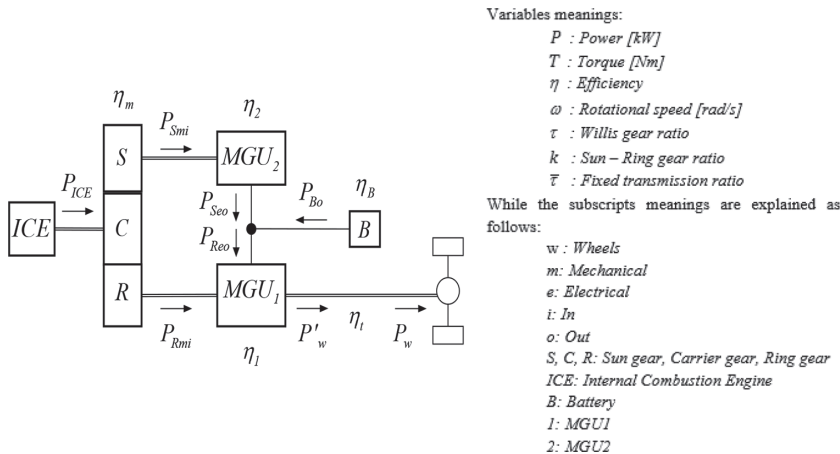


Figure 2: Power flow scheme of CVT architecture.

The analysis carried out in this study, due to the limited influence of the inertial terms of the planetary gear train components on the overall efficiency, does not consider these terms. Thus, the equations shown below are only algebraic equations and are to be considered as a stationary model.

$$\tau = \frac{\omega_R - \omega_{ICE}}{\omega_S - \omega_{ICE}}$$

where:

$$\tau = \frac{z_S}{z_R}$$

$z_S$  and  $z_R$  represent the sun and ring teeth number, in particular  $z_R$  is conventionally a negative number because the teeth are internal.

In this study,  $z_S$  and  $z_R$  are chosen as, 30 and  $-78$ , respectively.

Some fundamental relationships, which will be used in the model construction, are shown below:

$$\begin{cases} T_{ICE}\eta_m = T_{smi} + T_{Rmi} & \text{torque balance at the jo int} \\ P_{ICE}\eta_m = P_{Smi} + P_{Rmi} & \text{power balance at the jo int} \\ \left(1 - \frac{1}{\tau}\right)\omega_{ICE} = \omega_S - \frac{1}{\tau}\omega_R & \text{Willis formula} \end{cases}$$

By conveniently combining the above equations, it results:

$$T_S = -\tau T_R$$

From which:

$$T_{ICE} = \frac{\left(1 - \frac{1}{\tau}\right)}{\eta_m} T_S$$

On the basis of the three following equations, once the value of  $k$  has been chosen, it is possible to obtain a relationship between the mechanical ring gear power and the mechanical sun gear power.

$$\begin{cases} T_S = -\tau T_R \\ P_{Smi} = \omega_S T_S \\ P_{Rmi} = \omega_R T_R = -\frac{\omega_R}{\tau} T_S \end{cases} \rightarrow \frac{P_{Smi}}{P_{Rmi}} = -\tau k$$

where:

$$k = \frac{\omega_S}{\omega_R}$$

Two different mathematical models of the vehicles described were implemented on MATLAB Simulink.

3 ICE AND ELECTRIC COMPONENT EFFICIENCY

It is of primary importance, as previously stated, to properly address the losses in the main components in order to effectively compare the two architectures. One referred to (G. Pellegrino, A. Vagati, P. Guglielmi and B. Boazzo) for losses modeling of the motor-generators (Fig. 3 (G. Pellegrino, A. Vagati, P. Guglielmi and B. Boazzo)).

Torque, speed and losses were normalized with the aim of referring these values to the same type of electric machines (interior permanent magnet synchronous motor) characterized by similar, but not equal, rated power as proposed by (G. Pellegrino, A. Vagati, P. Guglielmi and B. Boazzo).

Thanks to this procedure, the electrical loss contour map in Fig. 3, once normalized, can be used both for  $MGU_1$  and  $MGU_2$ .

The efficiency map related to the inverter presented in (Hyeokjin Kim, Hua Chen, Jianglin Zhu, Dragan Maksimovic and Robert Erickson) is shown in Fig. 4. From these values, one can compute the consequent losses and their corresponding values for a 650 DC link voltage by interpolation.

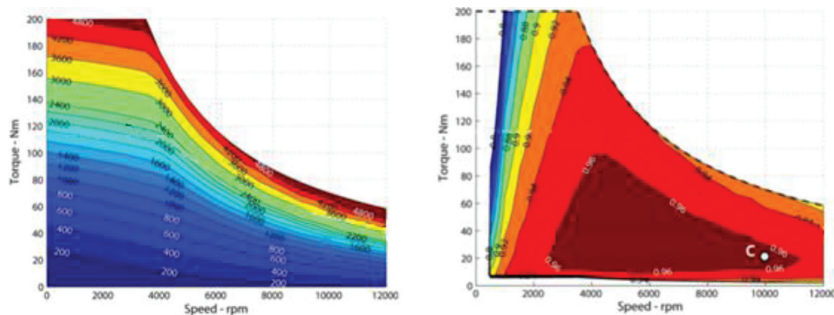


Figure 3: Efficiency and loss contour map for a 73 kW interior permanent magnet synchronous motor (G. Pellegrino, A. Vagati, P. Guglielmi and B. Boazzo).

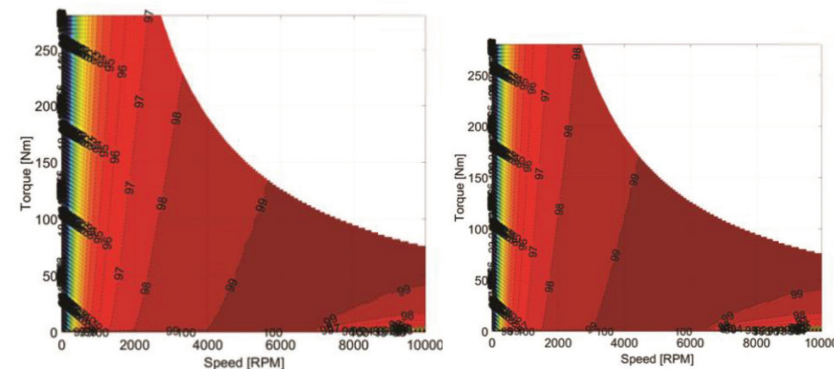


Figure 4: Sic Inverter efficiency for a 350 DC voltage and 800 DC voltage, respectively (Hyeokjin Kim, Hua Chen, Jianglin Zhu, Dragan Maksimovic and Robert Erickson).

Therefore, the approximating loss functions are:

$$\begin{cases} \text{Losses}_{[w]} = 2.5T_{[Nm]}^{1.18} & \text{for } n_{[rpm]} < 6000 \\ \text{Losses}_{[w]} = 2.5T_{[Nm]}^{1.18} + 350 \left( \frac{n_{[rpm]} - 6000}{4000} \right)^2 & \text{for } n_{[rpm]} > 6000 \end{cases}$$

The losses in the battery were estimated from the experimental data available at the mechanical engineering department of the University of Genoa (DIME). As far as the DC/DC converter (necessary to connect the battery to the DC link) is concerned, a constant efficiency value equal to 0.97 has been considered.

Accurately evaluating the losses in this component would need an in-depth study; however, this is not relevant to the objectives of this study. As a matter of fact, the power flowing out and in the storage system is the same, and both of the structures analyzed have the same DC/DC converter, hence the same losses associated with each. In addition, given the architecture taken in consideration (parallel), large variation of these two components efficiency slightly affects the overall fuel economy.

On balance, the comparison between the two architectures would not be altered by any errors in the modelling of either the DC/DC converter or the storage system. Finally, as regards the internal combustion engine (ICE), a 72 kW petrol engine was chosen, its efficiency contour map is shown in Fig. 5 (Achim konigstein, Uwe Dieter Grebe, Ko Jen Wu, Per-Inge Larsson - Differenzierte analyse von downsizing- konzepten M.T.Z., 06/2008).

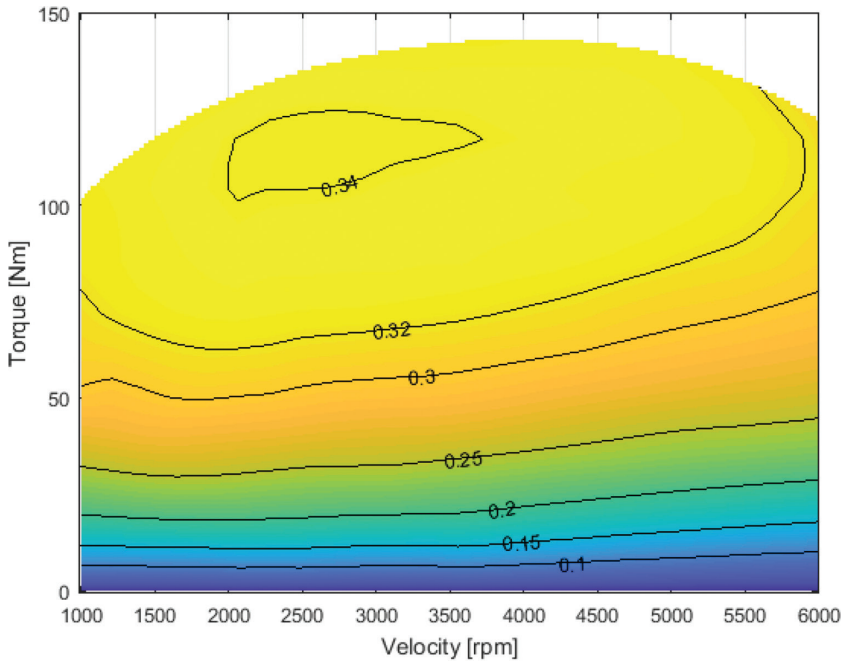


Figure 5: ICE efficiency map (Achim konigstein, Uwe Dieter Grebe, Ko Jen Wu, Per-Inge Larsson - Differenzierte analyse von downsizing- konzepten M.T.Z., 06/2008).

4 CONTROL LOGIC AND CVT OPTIMIZATION

The aim of the control logic implemented in the vehicle models is to instantaneously reduce fuel consumption in accordance with that presented in (Jinming Liu, Huei Peng).

This logic is simple if one looks at the DVT architecture, in that the goal is to maximize the ICE efficiency in every working condition. On the other hand, the CVT optimization process also has to take into account also the electrical losses caused by the power circulation between the two motor generator units.

A logical block scheme shows in Fig. 6 how to achieve the optimal transmission ratio  $k_{opt}$  for each couple of torque and speed (where  $k_{opt} = \omega_s / \omega_R$ ).

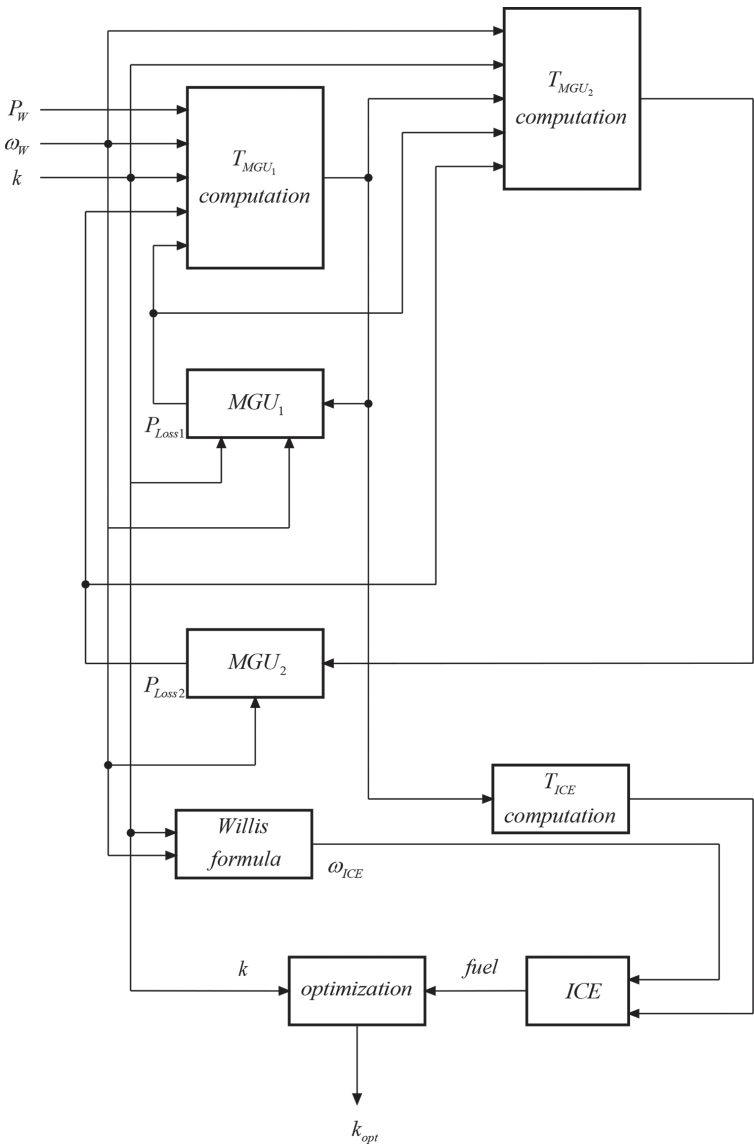


Figure 6: CVT optimization process.

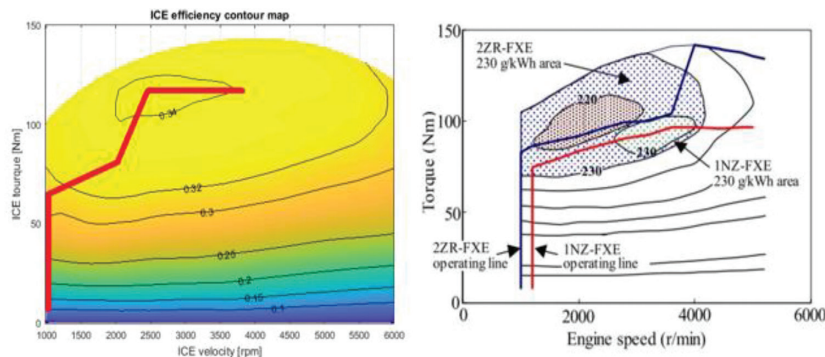


Figure 7: ICE working point deriving from CVT optimization (left), ICE working points declared by Toyota.

The effect of the optimization process regarding the choice of  $k_{opt}$  for each couple of torque and speed are visible in Fig. 7 where the ICE working points are highlighted with a red line. In particular, this result agrees with that presented by Toyota (Shouji ADACHI, Hikomasa HAGIHARA).

The transition from electric traction to ICE traction is a function of the state of charge (SOC) of the storage system; besides, it was chosen to charge the battery only through regenerative deceleration. All these logics were implemented the same way on the two vehicles in order to perform a valid comparison.

5 VEHICLE PARAMETERS AND ROAD MISSIONS

The US06, UDDS and HWFET cycles allow an immediate comparison of the results obtained in this study with those already available in the scientific literature but their drawback is given by being characterized by constant slope.

Therefore, three extra missions were simulated, whose data were experimentally acquired; two of them take place in the city of Genoa (urban mission and fast urban mission) and the third takes place around Genoa in the countryside (extraurban mission).

The main parameters related to all the missions simulated are listed in Table 1, while the main feature of the vehicles taken into consideration are reported in Table 2.

Table 1: Road mission main parameters.

	Average speed [kph]	Maximum speed [kph]	Length [km]	Change of altitude <sup>1</sup> [m]	Maximum road slope [%]
US06	78	130	13	-	-
UDDS	31	90	12	-	-
HWFET	78	97	16.5	-	-
Urban	24	57	11.4	20	negligible
Fast urban	27	68	22	62	6
Extra urban	45	80	36	300	9

<sup>1</sup>The starting altitude is the same as the final altitude, thus the positive change of altitude is intended which equals then the negative.

Table 2: Vehicle data.

Mass [kg]	1450
Rolling coefficient	0.01
Aerodynamic coefficient	0.25
Front section [m <sup>2</sup> ]	2.3
Wheel radius [m]	0.3
Final gear ratio	3.45/10.8
Final gear ratio efficiency	0.97
Planetary gear train/DVT efficiency	0.95/0.97
Air density[kg/m <sup>3</sup> ]	1.22
ICE maximum power [kW]	72
ICE maximum torque [Nm]	142
MGU <sub>2</sub> maximum torque [Nm]	163
MGU <sub>2</sub> base speed <sup>2</sup> [rpm]	3000
MGU <sub>2</sub> maximum speed [rpm]	17000
MGU <sub>1</sub> maximum torque [Nm]	43
MG <sub>1</sub> base speed [rpm]	5000
MG <sub>1</sub> maximum speed 10000 [rpm]	1000
DC link voltage [V]	650

## 6 SIMULATION RESULTS

Observing the fuel consumption results over the different missions simulated would be sufficient to identify the most efficient solution; however, in order to understand the motivation that lies beneath, one must also take into consideration the average ICE efficiency and the electrical losses.

The ICE working points are represented both for CVT and DVT architectures, in particular the points in Fig. 8 are given by urban mission and the points in Fig. 9 represent extra urban mission.

From a quick look, it is easy to notice that the DVT not being able to continuously vary the transmission ratio forces the ICE to work in a broader area even in zones distant from the optimal efficiency line. On the contrary, this line is easily followed by the CVT architecture.

Consequently, the average ICE efficiency is 3% higher in the CVT system than in the DVT structure as reported in Table 3. Despite this fact, the electrical losses due to the realization of the transmission ratio (electrical losses due to electric traction and regenerative deceleration are not included) cancel the benefit given by the thermal generation efficiency increase: the amount of these losses goes from 20% to 13% (depending on the mission type) of the energy generated by the engine.

Thus, thanks to the CVT structure, the engine is able to work at higher efficiency values, but the electrical losses deriving from the electrical power necessary to make this operation possible penalize the overall power train energy efficiency.

The fuel economy, average ICE efficiency and electrical loss values deriving from the missions simulated are reported in Table 3.

<sup>2</sup>Note that the DVT architecture is characterized by the presence of only one electric motor, here supposed to be identical to MGU<sub>2</sub>.



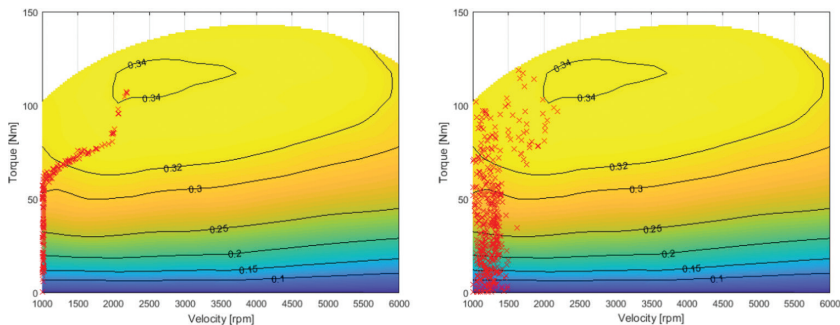


Figure 8: Urban mission ICE working points: CVT (left), DVT (right).

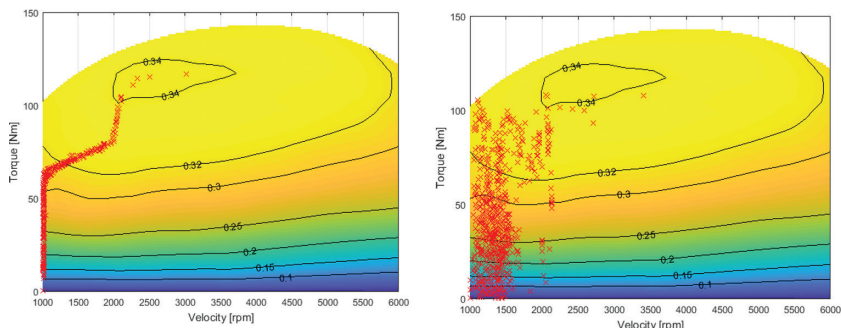


Figure 9: Extra urban mission ICE working points: CVT (left), DVT (right).

Table 3: Fuel economy, ICE efficiency and electrical losses on different missions

	Fuel economy [kpl]		Average ICE efficiency		Electrical losses <sup>3</sup> [%]	
	CVT	DVT	CVT	DVT	CVT	DVT
US06	15.7	17.4	0.34	0.305	17	-
UDDS	21.3	23	0.3	0.27	15	-
HWFET	21.6	23.7	0.32	0.27	21	-
Urban	24.5	25.3	0.28	0.25	13	-
Fast urban	25	26.6	0.3	0.275	13	-
Extra-urban	26.7	29.3	0.3	0.27	15	-

It is easy to notice that DVT structures allow a fuel saving from 5% to 10% compared to CVT solutions. In particular, the difference in fuel economy is higher in high-speed missions (highways), where CVT transmission in order to optimize the overall efficiency needs a superior current to flow from MGU<sub>2</sub> to MGU<sub>1</sub> and thus generating anyway higher electrical losses.

<sup>3</sup>The electrical losses here considered are only the ones associated with the realization of the variable transmission (they are therefore absent in the other architecture). Their amount is given in percentage with respect to the ICE generated energy.

This increase in electrical losses during high-speed situations can be found in Table 3 looking at US06 and HWFET results.

## 7 CONCLUSIONS

Two different hybrid parallel architectures were analyzed and their mathematical models were created and implemented on MATLAB Simulink. The various road mission simulations showed how the CVT architecture is able to increase the thermal efficiency but only at the cost of high electrical losses; in particular, the amount of these losses is not sufficiently balanced by the first advantage achieved.

It is interesting to notice that electrical losses associated with the continuously variable transmission are significantly higher in high-speed mission, and in particular, their entity is comparable to the electrical losses due to deceleration energy recovery plus those related to electric traction.

On the basis of this study, even if it provides a higher driving comfort, architectures based on the continuously variable transmission (currently the best-selling technology) do not seem to represent the optimal energy solution.

## REFERENCES

- [1] Mahmoudi, A., Soong, W.L., Pellegrino, G. & Armando, E., Efficiency maps of electrical machines. *2015 IEEE Energy Conversion Congress and Exposition (ECCE)*, pp. 2791–2799, 2015.  
<https://doi.org/10.1109/ecce.2015.7310051>
- [2] Burress, T.A., Coomer, C.L., Campbell, S.L., Seiber, L.E., Marlino, L.D., Staunton, R.H. & Cunningham, J.P., *Evaluation of the 2007 Toyota Camry Hybrid Synergy Drive System*, ORNL/TM- 2007/190, UT-Battelle, Oak Ridge National Laboratory, Oak Ridge, Tennessee, 2008.
- [3] Burress, T.A., Coomer, C.L., Campbell, S.L., Wereszczak, A.A., Cunningham, J.P. & Marlino, L.D., *Evaluation of the 2008 Lexus LS 600h Hybrid Synergy Drive System*, ORNL/TM-2008/185, UT-Battelle, Oak Ridge National Laboratory, Oak Ridge, Tennessee, 2009.
- [4] Burress, T.A., Campbell, S.L., Coomer, C.L., Ayers, C.W., Wereszczak, A.A., Cunningham, J.P., Marlino, L.D., Seiber, L.E. & Lin, H.T., *Evaluation of the 2010 Toyota Prius hybrid synergy drive system*. Oak Ridge National Laboratory (ORNL); Power Electronics and Electric Machinery Research Facility, Technical Report ORNL/TM2010/253.
- [5] Pellegrino, G., Vagati, A., Guglielmi, P. & Boazzo, B., Performance comparison between surface-mounted and interior PM motor drives for electric vehicle application. *IEEE Transactions on Industrial Electronics*, **59**(2), pp. 803–811, 2012.  
<https://doi.org/10.1109/tie.2011.2151825>
- [6] Kim, H., Chen, H., Zhu, J., Maksimovic, D. & Erickson, R., Impact of 1.2kV SiC-MOSFET EV traction inverter on urban driving. *2016 IEEE 4th Workshop on Wide Bandgap Power Devices and Applications (WiPDA)*, Fayetteville, AR, pp. 78–83, 2016.
- [7] Königstein, A., Grebe, U.D., Wu, K.J. & Larsson, P.-I., Differenzierte analyse von downsizing- konzepten. *MTZ - Motortechnische Zeitschrift*, **69**(6), pp. 468–476, 2008.  
<https://doi.org/10.1007/bf03227458>
- [8] Liu, J. & Peng, H., *Control Optimization for a Power-Split Hybrid Vehicle*. Proceedings of the 2006 American Control Conference, Minneapolis, Minnesota, USA, 2006.

- [9] Adachi, S. & Hagihara, H., TOYOTA MOTOR CORPORATION, AICHI JAPAN The renewed 4-Cylinder Engine Series for Toyota Hybrid System.
- [10] Liu, J., Peng, H., & Filipi, Z, *Modeling and Control Analysis of Toyota Hybrid System*. Proceedings, 2005 IEEE/ASME International Conference on Advanced Intelligent Mechatronics, pp. 134–139, 2005.